EFFECTS OF ELECTRODE MATERIAL ON ELECTRODE EROSION OF ELECTRICAL DISCHARGE MACHINING DRILL

By

GARNER COPHER

Bachelor of Science in Mechanical Engineering

Bachelor of Science in Aerospace Engineering

Oklahoma State University

Stillwater Oklahoma

2019

Submitted to the Faculty of the
Graduate College of the
Oklahoma State University
in partial fulfillment of
the requirements for
the Degree of
MASTER OF SCIENCE
May, 2021

EFFECTS OF ELECTRODE MATERIAL ON ELECTRODE EROSION OF ELECTRICAL DISCHARGE MACHINING DRILL

Thesis Approved:

Dr. Kurt Rouser

Thesis Adviser

Dr Sandip Harimkar

Dr. Jamey Jacob

ACKNOWLEDGEMENTS

The Author would like to thank Dr. Rouser, Dr. Harimkar, and Dr. Jacob for their assistance, guidance, and support of this study. The author would also like to thank the research assistant Daniel Velasco for the assistance of running experiments and data collection.

Name: GARNER G. COPHER

Date of Degree: MAY, 2021

Title of Study: EFFECTS OF ELECTRODE MATERIAL ON ELECTRODE EROSION OF ELECTRICAL DISCHARGE MACHINING DRILL

Major Field: MECHANICAL AND AEROSPACE ENGINEERING

Abstract: This paper presents an experimental investigation of the effects of electrode material and workpiece material on electrode wear and performance of a handheld electrical discharge machining drill. In the aerospace maintenance, repair, and overhaul industry, large quantities of high strength fasteners must be removed. These fasteners are difficult to remove and take up a significant amount of time when using traditional methods with mechanical twist drill bits. Electrical discharge machining has become a well-developed technology in the last century, utilizing pulsed electrical arcs to erode target material. Perfect Point EDM has developed a handheld drill configuration of an electrical discharge machining drill named "E-Drill™" to speed up the fastener removal process. While the electrical discharge machining process is active, the discharging electrode is eroding along with the target material. Previous work has addressed the erosion process, and erosion prediction algorithms have been developed to aid the machine in estimating cut depth, when to replace the electrode and supply chain management. This current investigation involves experiments with an E-Drill™, in which copper and brass electrodes were used to cut into Inconel and titanium alloys to measure and calculate electrode wear and performance parameters. These parameters include cut time, cut rate, electrode volume ratio, and volume removal rate. The brass electrodes consistently produced cut times of 40s to 50s for both workpiece materials as opposed to 145s to 245s for copper. The brass electrode volume ratio, which is the ratio of lost electrode volume to volume of target material removed, was more than twice that of copper for either workpiece material, however, the copper appeared to be affected more drastically by the workpiece material than the brass electrodes.

TABLE OF CONTENTS

Chapter Page

Chapter Page

LIST OF TABLES

Table Page

LIST OF FIGURES

Figure Page

CHAPTER I

INTRODUCTION

1.1 Motivation

In the aerospace maintenance, repair, and overhaul (MRO) industry, oftentimes various permanent fasteners must be removed. Such fasteners include locking studs, locking threaded inserts, rivets, and other types of locking fasteners, two fasteners of the key locking type can be seen in fig 1. There is great diversity in the type of material chosen for these fasteners, therefore, a wide variety of material properties and performances exist. When a certain machine or system is being designed, the fasteners in use would be chosen based on the required strength properties. But over time, some of the fasteners may need to be replaced or removed due to various factors. The fastener may be in a high cyclic loading condition, in high static shear or tension, or could have sustained damage, amongst other occurrences. The strength and reliability that is offered by these types of fasteners also means that it can be very time consuming and challenging to remove them. These challenges are then compounded upon when the materials in use are high strength, or when tight tolerances are in place such as in aerospace applications. Traditionally, a removal process would consist of drilling out the fastener with a drill bit and removing the remaining pieces once the locking mechanism is broken. This traditional process, although simple, has its own limitations. If the fastener material has a high hardness, the tools

used must be more robust, the user must apply more pressure, the chance of part damage increases, and usually the removal time is extended. The MRO industry is greatly impacted by repair cost and time. When considering the large number of repairs that must be made, even small improvements to a process can yield a significant increase in productivity and profits.

Figure 1: Key-locking stud and insert

A potential solution to the above repair dilemma is electrical discharge machining (EDM) drilling, specifically the handheld variety. The EDM process uses pulsed electrical arcs to erode the material that needs removal. There is a specific shaped electrode attached to the tool that delivers the electric current to "drill" a hole into a shape that mirrors the electrode. In the case of this study, the electrode shape is a hollow cylinder. A consequence to the EDM process is the electrode is consumed through the same erosion process. The electrode also delivers dielectric fluid to aid in the process. The dielectric fluid acts as a coolant, a means to flush away debris from the workpiece and electrode, and an insulator to allow proper voltage to build before an arc is formed. This EDM drill has many benefits. Because it is using electricity to remove material, metals with high hardness levels, and that are traditionally difficult to machine, can be easily cut.

There is zero tool pressure because there is theoretically no contact between the electrode and working material. Finally, the debris should be entirely contained in the dielectric fluid instead of metal shavings contaminating the workspace. EDM is a widely used process and can be found in many industries such as medical, automotive, and die manufacturing.

Perfect Point EDM (PP EDM) E-Drill™ has developed a handheld EDM drill that shows great potential for aerospace fastener removal. The E-Drill™ system has a proprietary electrode wear prediction code that is fully integrated into the user interface. When the operator inputs the fastener type, head shape, electrode diameter and cut depth, the prediction code gives the user an indication as to when it is time to change the electrode. Different example electrode diameters are shown in fig 2. This prediction model is how the machine determines how deep the electrode is cutting. The cut depth prediction is a challenging aspect because as the hole is being drilled, the electrode is also shrinking. This prediction model is a complex system, yet there are still many variables at play that need further investigation. Figure *3* simply illustrates the E-Drill™ in use during the wear study.

Figure 2: Some various electrode diameters

Figure 3: Illustration of E-Drill during use (left), finished cut (right)

1.2 Goals and Objectives

This study serves to investigate the effects and relationship between electrode material, workpiece material, and electrode wear. Cuts will be made with electrodes made of pure copper, and standard free machining brass. The parent materials that are to be cut upon are titanium and Inconel alloys. Three cuts will be made of each material combination resulting in twelve total cuts at a constant cut depth. The electrode wear results will be compared against a stock electrode wear study to determine any effects of the above stated test parameters. The primary goals of this study are 1) to evaluate the electrode performance through wear ratios, cut times, and cutting rates, 2) compare electrode wear behavior and performance of the two alternative electrode materials to the stock electrodes, and 3) assess the possible correlation of electrode wear to the material properties of both the electrode and the parent material.

CHAPTER II

BACKGROUND

This chapter presents a summary of the various types of EDM technology in use, previous studies done on EDM, and typical methods used for measuring electrode performance and wear.

2.1.1 Electrical Discharge Machining Overview

In the 1770s the EDM erosion effect was discovered, but it wasn't until 1943 that Russian scientists were able to harness its potential into a useful tool. Since then, EDM technology has evolved into a well-established method and allows for the machining of materials that are otherwise challenging to machine using traditional mechanical methods. Material mechanical properties such as hardness, ductility, and thermal conductivity limit the machinability of materials when using traditional tools like lathes, drills, and mills. EDM does not suffer from the same limitations as these traditional tools. The basic components of the EDM process are the machine itself, the electrode, the dielectric fluid, and the workpiece. The machine can be of the wire EDM, die sinker EDM, or EDM drill varieties depending on the application. The electrode is the part that is doing the actual cutting of the workpiece. These electrodes can come in many shapes, sizes, and materials. Wire EDM uses an electrode that is a continuous wire, die sinker EDM uses an electrode that is a more complex shape to "stamp" a part, and EDM drill electrodes are typically a hollow or solid cylinder. In the case of this study, the E-Drill™ uses a

hollow cylinder electrode. According to EDM Tips [8] the dielectric fluid is used to submerse and insulate the electrode from the workpiece until a voltage in the range of 50 - 300volts is developed. Common dielectric fluids are often petroleum-based liquids such as kerosene, however, deionized water can be used and is what the current study utilizes. The EDM erosion occurs from the arcs that form in the gap between the workpiece and electrode. Each arc erodes a small amount of the workpiece by quickly melting it and flushing it away in the dielectric liquid. When these arcs occur quickly enough, a smooth drilling effect is achieved.

2.1.2 Wire EDM

Wire EDM uses the same underlying mechanisms to erode the workpiece, however the electrode in use is a continuous wire. Figure 4 illustrates a simple wire EDM machine in use. The wire electrode is constantly eroding away, so a spool of wire is continuously feeding in new electrode material. According to *All About EDM* [13] this constant wire feed allows wire EDM to retain consistent cutting characteristics since the electrode experiences minimal wear. Because the wire is all the way through the workpiece, hard materials may be used to create complex parts much like what standard machining can produce.

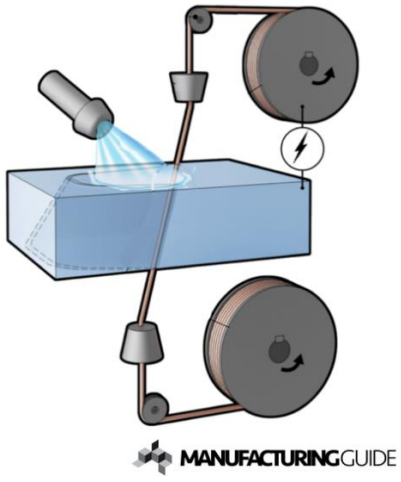

Figure 4: Wire EDM illustration [2]

2.1.3 Die Sinker EDM

Figure 5 illustrates a die sinker EDM machine. Die sinker EDM is also referred to as "ram EDM" since the electrode is "rammed" into the workpiece. The electrode used in this process is usually of complex geometry and the "negative" equivalent of what the end product should be. Figure 6 shows an example of a ram EDM electrode, and the part that it can produce. Molds and dies are common products produced through ram EDM.

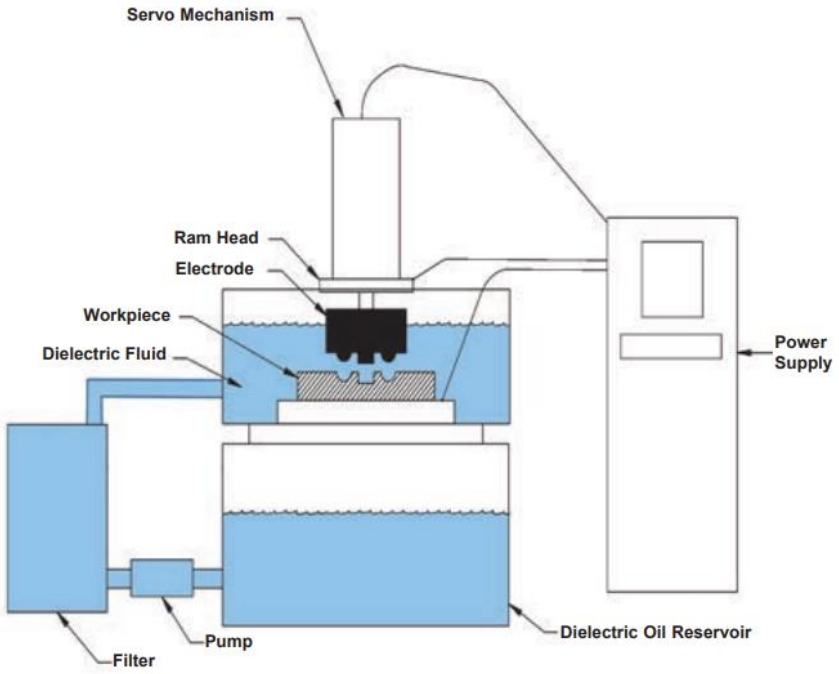

Figure 5: Ram EDM illustration [20]

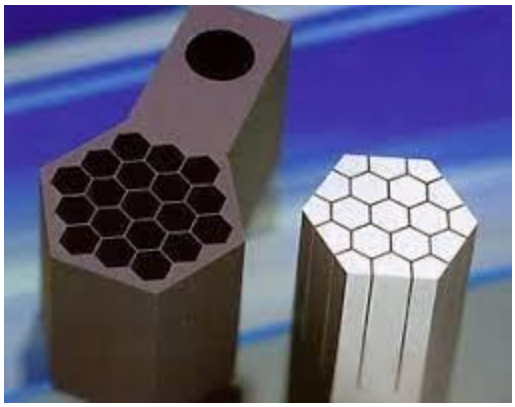

Figure 6: Ram EDM electrode example [20]

2.1.4 EDM Drill

Figure 7 shows an EDM drill machine during operation and fig 8 shows some examples of electrodes used and holes that can be drilled. EDM drilling is used for micro holes of diameters less than 3mm. The way this works is very similar to ram EDM in the sense that the electrode is "rammed" into the workpiece, except it is used to create a through hole. For holes of this scale and high aspect ratio, traditional twist drill bits present challenges caused by the strength of the bit itself. But in the case of micro EDM drilling, there is no normal force between the electrode and workpiece so the physical strength of the electrode is not an important factor.

Figure 7: Typical EDM drill [10]

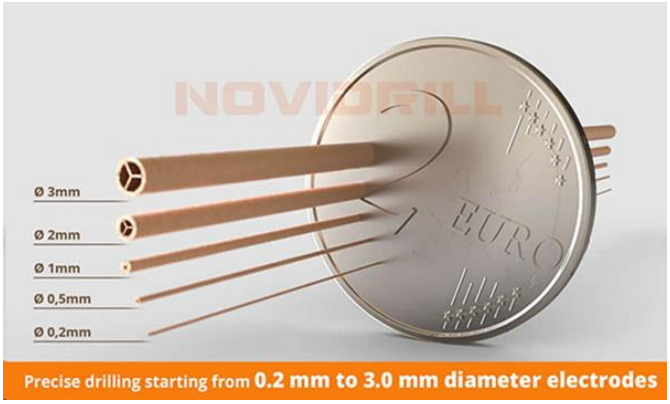

Figure 8: EDM drill electrode sizes [9]

2.1.5 E-Drill™

Perfect Point EDM (PPEDM) has developed a novel EDM hand drill named "E-Drill™" shown in fig 9. Similar in function to ram EDM and EDM drilling, the E-Drill™ uses a special electrode to drill a hole by "ramming" the electrode into the workpiece. This drill is in a handheld formfactor, which allows for higher portability, mobility, and can be adapted to many work surfaces. The E-Drill™ has been designed primarily for the use of fastener removal. Because of the special purpose, the electrodes are hollow tubes specifically designed to remove special aerospace fasteners. These electrodes are also quick to replace on the drill because one end is threaded so that it may be screwed into place. There are various electrode diameters available, and the diameter selection is dependent on the required task. The hollowed center of the electrodes allows the dielectric fluid to flow to the workpiece where it cools, flushes, and insulates during each cut. The mobility of the E-Drill ™ makes it suitable for repairs on large objects or objects of unusual shape, where they cannot fit inside a typical EDM machine. A key component of the E-Drill™ is the locator shown in fig 10. The locator is used to help keep the drill perpendicular to the workpiece, and it also has a red gasket to form a watertight seal at the interface between the workpiece and drill. This seal allows the electrode to remain submerged in water while cutting.

Figure 9: Perfect Point EDM E-Drill system (Courtesy of PPEDM)

Figure 10: E-Drill locator and red gasket (Courtesy of PPEDM)

2.2 Previous Research

There is a large and diverse pool of previously performed EDM research studies that cover many different aspects of EDM. These aspects include but are not limited to, types of EDM implementations, dielectric fluid studies, electric current and frequency analysis, and various performance measurement studies. Most of the previous studies are based on the more common EDM types like wire EDM, Ram EDM, and micro EDM drilling. Handheld EDM drilling is a young technology and there are not many studies when compared to the other common EDM types.

2.2.1 Micro EDM Electrical parameters

Gianluca D'Urso and Chiara Ravasio [18] studied the relationship between micro EDM electrode material, electrical parameters, cutting performance, and electrode wear. The experiment was performed by cutting 360 holes (90 per electrode) on a 1mm thick 316L stainless steel sheet using electrodes with diameters of 300μm and 120μm. The electrical parameters that were varied were voltage (95V, 110V, and 140V) and current (10A, 35A, 50A, and 80A) resulting in 5 electrode cuts per test condition. It was found that higher power exchange results in a faster material removal rate. The electrode materials that were compared were copper and tungsten carbide. The study showed that although copper can achieve higher material removal rates due to its low electrical resistance, it also suffers from faster wear, possibly from the lower melting point.

2.2.2 Micro EDM Electrodes and Electrical Parameters

Saad Mahmood Ali [5] studied the effects of electrode material and electrical process parameters. The electrode materials chosen were copper, graphite, zinc coated brass and tin coated copper. electrical parameters that were varied were pulse current (8A and 16A) and pulse on time (25μs and 75μs). The experiment was conducted by drilling into a test workpiece made of 304L stainless steel, which is commonly used in corrosive environments. The electrode cuts

were used to obtain data and then to attempt to form relationships to electrode wear. It was found that overall a higher pulse current resulted in better material removal rate and reduced hole taper, but also caused greater electrode wear. The electrode material that produced the greatest material removal rate was the pure copper electrodes, but the lowest electrode wear was produced by the graphite. This graphite result is likely due to the high melting temperature of graphite.

2.2.3 Micro EDM Electrode Material

Fu et al. [11] studied the effects of electrode material of a micro hole EDM machine. Using a Panasonic MG-ED-71 with 40μm diameter electrodes made of both pure tungsten and tungsten carbide, holes were drilled into 304L stainless steel test coupons. Along with the electrode material, the dielectric fluid was varied. Distilled water and EDM machining oil were the fluids used in the experiments. Throughout the experiment the electrode wear was monitored along with number of cuts made. The results from this study showed that the tool wear in EDM oil was much larger than in water, and tungsten carbide had much greater wear than the pure tungsten in both dielectrics.

2.2.4 Micro EDM Electrode Wear Prediction

Lee et al. [6] analyzed the effects of number of cuts and discharge time on micro EDM electrode wear. Using a commercial EDM drill EDB-435F of KTC Co. Ltd. 10 electrodes cut 10 identical holes each, resulting in 100 total cuts. They showed that electrode wear rates and ratios steadily increased, but quickly plateaued and remained somewhat constant. This was possibly caused by the electrode initial geometry changing until it was worn into a state of geometric equilibrium. Intuitively, this equilibrium is a state that all EDM processes should be able to achieve, therefore the longer the electrode is used, the more predictable it would become.

2.2.5 Ram EDM Dielectric Fluid

Niamat et al. [16] investigated how the dielectric fluid used affects material removal rate, electrode wear, and microstructures in die sinking EDM. The two dielectrics that were compared were kerosene and water. The electrical parameters that were varied were pulse-on-time (15μs, 30μs, and 45μs) and current (6A, 9A, and 10A). This resulted in 9 test cuts per dielectric fluid. Kerosene showed lower electrode wear, potentially due to excess carbon depositing on the electrode, reducing the wear rate. Water showed to have a lower parent material removal rate due to an arcing phenomenon when water rapidly decomposes under high electric current. The kerosene also resulted in a smoother surface finish than the distilled water, possibly because the material removal process in water relies more upon melting and crack propagation as opposed to kerosene which relies on melting and vaporization.

2.2.6 Hybrid EDM Electrode materials

Ahmed et al. [4] studied electrode wear properties of brass, copper, and copper tungsten electrodes in a hybrid EDM machine. The hybrid EDM includes a DC power supply in addition to the typical pulsed electrical current that is used in EDM. Using an EDM drilling machine that has been outfitted with an additional DC power supply set to 50A. the idea being that the DC supply will allow the plasma channel to be maintained for a longer period of time, thus keeping the temperature elevated for longer. Experiments were executed using electrodes with an external diameter of 3mm, drilling through Inconel 718 plates with a thickness of 12.5mm. The study showed the pressure of the dielectric fluid influenced debris solidification on both the parent material and the electrode, with a lower pressure resulting in more solidification. The data also showed that the material removal rate was highest for the brass, and lowest for the copper tungsten. However, the electrode wear was highest for the copper, and lowest for the copper tungsten. This could be explained by the higher melting temperature of the copper tungsten

electrodes. However, there is still not a clear indication of why these electrodes could behave differently.

2.2.7 Micro EDM Surface Integrity

Hasc¸alık and C¸ aydas [12] investigated the finished surface integrity of EDM cuts into titanium alloy (Ti–6Al–4V) with variations in electrode material, pulse current, and pulse duration. Electrodes used were made of graphite, electrolytic copper, and aluminum. Using a FURKAN M25A die sinking EDM. Kerosene was the dielectric fluid used. The holes were cut to a depth of 5mm. The completed test cuts were polished, etched, and imaged with a scanning electron microscope. It was found that the recast layer in the specimens had extensive cracking, debris deposition, and a rough finish. The recast layer increased in thickness as the electric parameters were increased. Using the graphite and aluminum electrodes the cracking could be eliminated at 3A and 6A pulse currents, respectively. However, the copper created cracks regardless of cut settings.

2.2.8 E-Drill™ Electrode Wear Study

McCain [15] studied how electrode wear is affected by the cut depth, electrode diameter, and workpiece material. The motivation behind this study was to develop an electrode life prediction model to aid in electrode supply chain management. For example, if the number of cuts a single electrode could make could be accurately predicted, the electrode supply could be more accurately managed, possibly resulting in less surplus and saving money. This study used an E-Drill™ to drive copper alloy electrodes of varying diameters directly into Inconel and titanium test coupons at varying depths. These cuts and electrodes were then analyzed and used to create best fit curves, and finally a prediction model was created. The resulting prediction model produced promising results for cuts into Inconel and it was proposed that with more experiments, a far more robust and useful model could be made. On the other hand, the cuts into titanium produced highly varied results with many relative standard deviations over 100%. This was likely

caused by the electrode wear being very small, therefore any slag buildup on the electrode would have a significant impact on the standard deviation. This high variation resulted in the prediction model being unreliable with large errors. An unexpected result from the cuts into titanium was at the shallowest cut depth, the electrode showed negative wear. Meaning that the electrode gained mass throughout the duration of the cut. This gained mass must be coming from the titanium workpiece as there are no other possible sources of mass.

2.2.9 E-Drill™ Microstructure Study

After McCain's [15] findings of the electrodes gaining mass, Copher et al. [7] proposed that the electrodes may also be depositing onto the workpiece, so a plan to study the microstructure effects of the EDM drill was put in place. Many of the detrimental effects of EDM processes are at microscopic levels and need careful destructive sample preparation. It becomes extremely important to make sure that new defects from specimen preparation are not introduced in the sample. An illustration of the sample and where it came from can be seen in fig 11. First, specimens for microscopy were cut from the parent material workpiece specimens after electrode study cuts were made. Standard metallographic techniques [21] were used to prepare the samples [ASTM E3]. As most of the defects from EDM drilling are on nearby surfaces and hole walls, careful cross-sectional samples from the structures will be prepared using a custom low-speed, tungsten-carbide tipped cold saw blade. The samples with desired sections were mounted in Bakelite discs. Samples were carefully polished using a range of SiC polishing papers (with increasing fineness i.e. mesh size from 200 to 1200 mesh), diamond polishing (1 μm diamond size), and micro-cloth (with silica/alumina slurry down to 0.5 μm). To reveal the microstructure of the metallic samples, further etching of specimens using etchants for high temperature materials was performed. Suitable commercial etchants for high temperature aerospace materials include Adler's reagent.

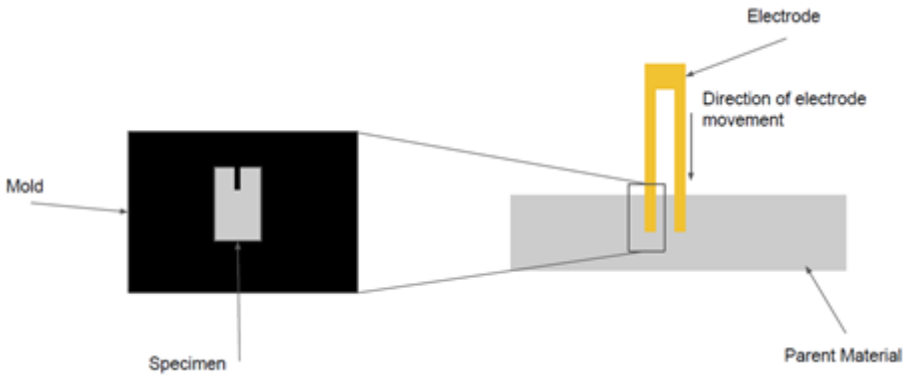

Figure 11: Illustration of microstructure sample

Polished and etched samples were imaged under optical and scanning electron microscope (SEM) to characterize defects such as recast layer, microstructural changes, and heat affected zones. The recast layer thickness was measured from SEM images. Microstructural effects such as grain size, grain distribution, and grain orientation in the recast layer were measured using SEM images. The standard linear intercept method was used to measure grain size. The rapid re-solidification of material in the parent metal often leads to precipitation of secondary phases. Due to differences in thermal expansion coefficient and lattice mismatch, the precipitation secondary phases often lead to formation of micro-cracks.

High magnification image (fig 12b) shows the microstructure in the parent material and the deposited debris. The parent material exhibits typical microstructure of Inconel with coarse matrix grains with grain size in the range of about 25-75 µm and some precipitation, likely of MC carbides, at the grain boundaries. There exists a distinct/sharp boundary between the deposited material and the parent material. The deposited material shows lamellae of extremely fine dendritic/cellular grains, indicating rapid solidification of molten droplets as the source of formation. The grain boundaries appear cleaner in the deposited material likely to due to dissolution of carbides in the melt. Micro-cracks are observed in the deposited (re-solidified) material. The microcracks appear to originate between the dendritic grains in the deposited

material and reach the interface with some cracks reaching the grain boundaries of the parent material. Micro-porosity is also observed in the deposited material.

In addition to the deposited debris (fig 12b), the parent material showed formation of recast layer (figs 12c and 12d). The recast layer has variable thickness along the length of the trench, with a thickness range of about 20-100 μm. The surface of the recast layer showed microcracks (fig 12c). At some places, the cracks originated inside the recast layer and reach into the parent material at grain boundaries (fig 12d). Note that grain boundaries in the parent material have hard precipitates and are highly susceptible to cracking. The recast layer exhibits highly refined dendritic/cellular grains characteristic of rapid solidification. In selected regions of the recast layer, some grains show distinctly differing contrast (i.e. dark and bright grains in fig 12d). The differing grain contrast could be due to distinctly different orientation or composition of the grains. It is possible that the wear and melting of EDM electrode leads to incorporation of copper in the recast layer, and thereby, significantly altering the composition of the recast layer.

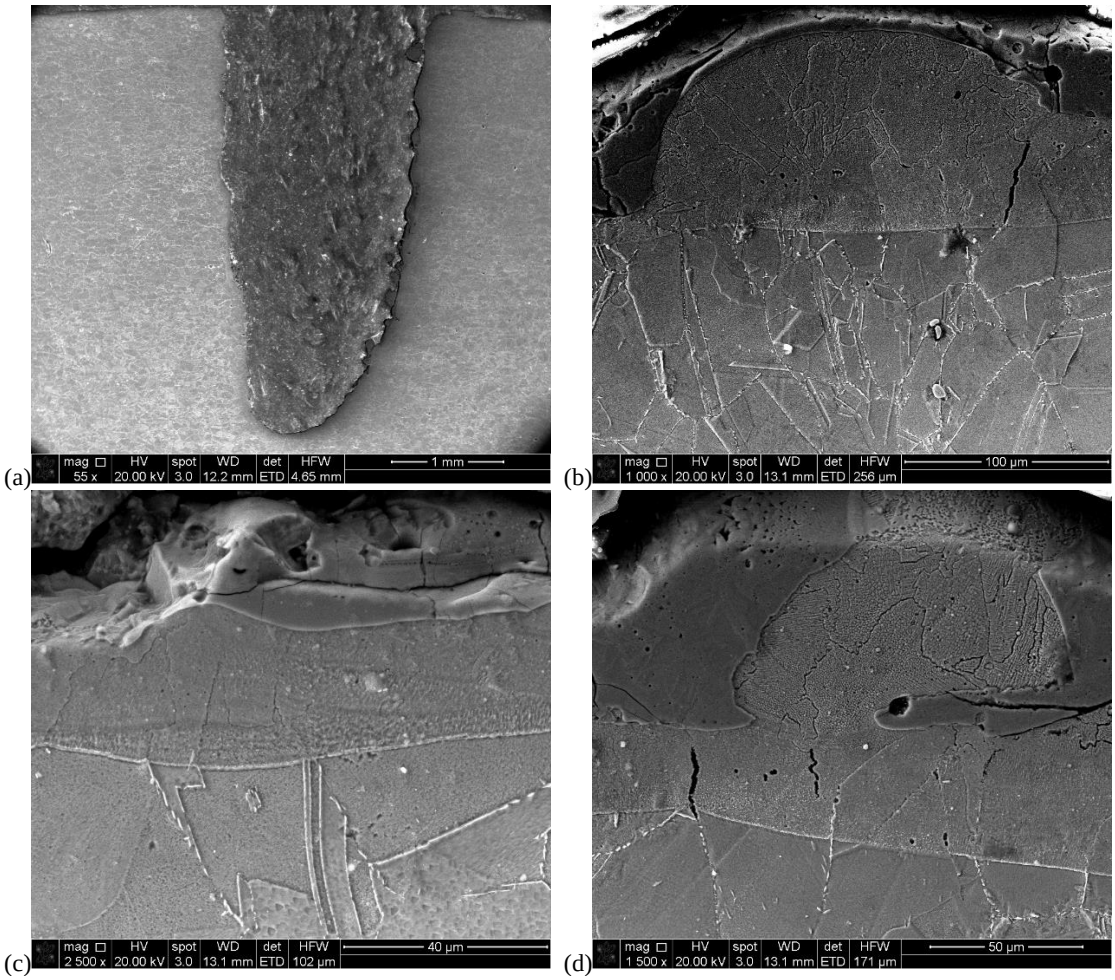

Figure 12: SEM micrographs of electrode wear study for Inconel.

Low magnification image fig 13a shows the EDM machined trench in Titanium alloy. The width of the machined trench is relatively uniform. The machined surface is relatively rough and covered with recast layer. Compared to Inconel specimens, the cracking of recast layer in the Titanium alloys sample was extensive. The fracture and delamination of the recast layer can be clearly seen near the base of the machined trench.

The recast layer with thickness of up to 50 µm was observed. It consisted of refined dendritic/cellular grains consistent with the rapid solidification molten material of the workpiece fig 13b. The rapid re-solidification occurs in multiple layers due to ejection and flushing of

molten material as the EDM machining progresses, resulting in distinct layers of dendritic structure in the recast layer. The orientation of dendrite growth also changes in the re-solidified layer indicating complex phenomena related to heat flow and melt flow dynamics. At many regions, the recast layer is extensively cracked fig 13c. Both vertical through-thickness cracks and lateral interfacial cracks were observed, causing disintegration of the recast layer from the parent material.

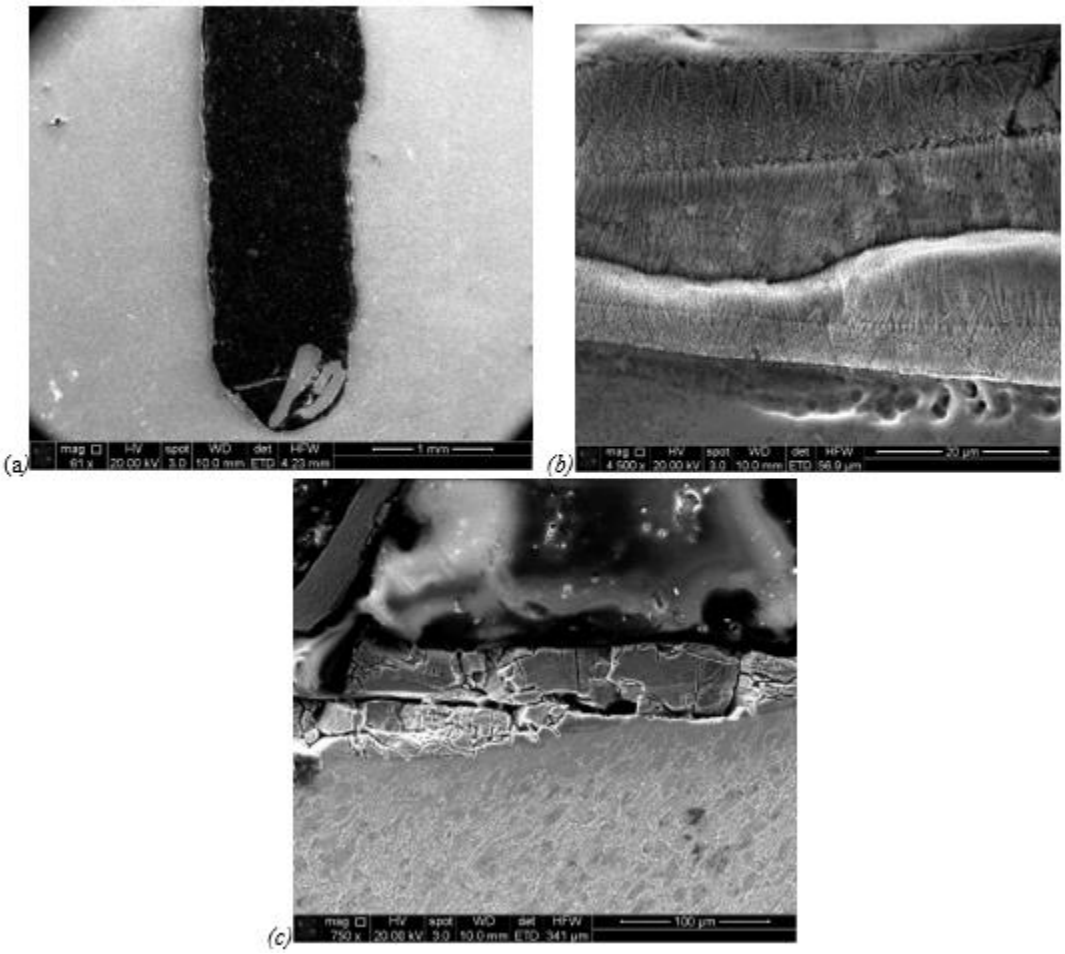

Figure 13: SEM micrographs of electrode wear study for titanium.

After the microstructure study indicating that the electrode was depositing onto the workpiece, the possibility of a different electrode material having an impact on that mechanism was reached, leading to the current electrode material study.

2.3 Theory of Analysis

This study focuses on 4 key electrode erosion performance parameters. These parameters are cut time (t), cut rate (μ_h), volume removal rate(μ_v), and volume removal ratio (ζ). Cut time (t) is measured automatically and displayed on the user interface of the E-Drill™. The cut time is important because it is directly used to calculate some of the other parameters mentioned, and it is also the quickest and simplest way to directly compare electrode efficacy. The cut rate is the measured cut depth divided by cut time. this can be used to determine a process time for a particular repair. Volume removal rate is the volume of material removed from the workpiece material divided by cut time. This is done by measuring the amount of mass lost into volume through the material specific volume. Finally, the volume removal ratio, is the volume of electrode lost divided by the volume of workpiece material removed.

$$\mu_h = \frac{h}{t} \tag{1}$$

$$\mu_v = \frac{V}{t} \tag{2}$$

$$\zeta = \frac{(\Delta m_e)(v_{s_{Pe}})}{(\Delta m_P)(v_{s_{PP}})} \tag{3}$$

CHAPTER III

EXPERIMENTAL METHODOLOGY

3.1 Experiment Setup

The facility in which this study was performed is Oklahoma State University Richmond Hill Research Facility. It houses all tools, machines and safety equipment needed to execute the necessary experiments safely and effectively. The E-Drill™ is connected to a 240V outlet on a circuit dedicated to the machine making it electrically isolated from other outlets. The room the E-Drill™ is in is somewhat secluded from the rest of the facility, and it is that room's only purpose. This makes it easy to keep unqualified individuals from being in contact with the machine and materials.

Two electrode materials, copper and brass will be evaluated in this study. Due to the differing material properties there is potential for different electrode performance. Brass has roughly 70% lower thermal conductivity, 340% higher electrical resistivity, and nearly 300°F lower melting temperature when compared to copper [1]. This study can bring to light possible process optimization, whether it be through specific electrode to workpiece matching, or through overall EDM optimization. The electrodes being used are approximately .315" in outside diameter and 1.26" in length.

The test coupons are 2.5 in squares, .25in thick, made from Inconel 718, and titanium (Ti-6Al-4V), some examples of test coupons before and after cuts can be seen in fig 14. These materials are often found in modern jet engines. The Inconel is often found in the hot section of the jet engine due to its ability to retain its strength in high temperatures and the titanium is often found in the cold section of the engines because of its high strength and low weight. These metals are difficult to machine through traditional methods. The metals' hardness, strength, and thermal properties negatively impact mechanical machining performances and thus require special tooling to properly cut at reasonable rates.

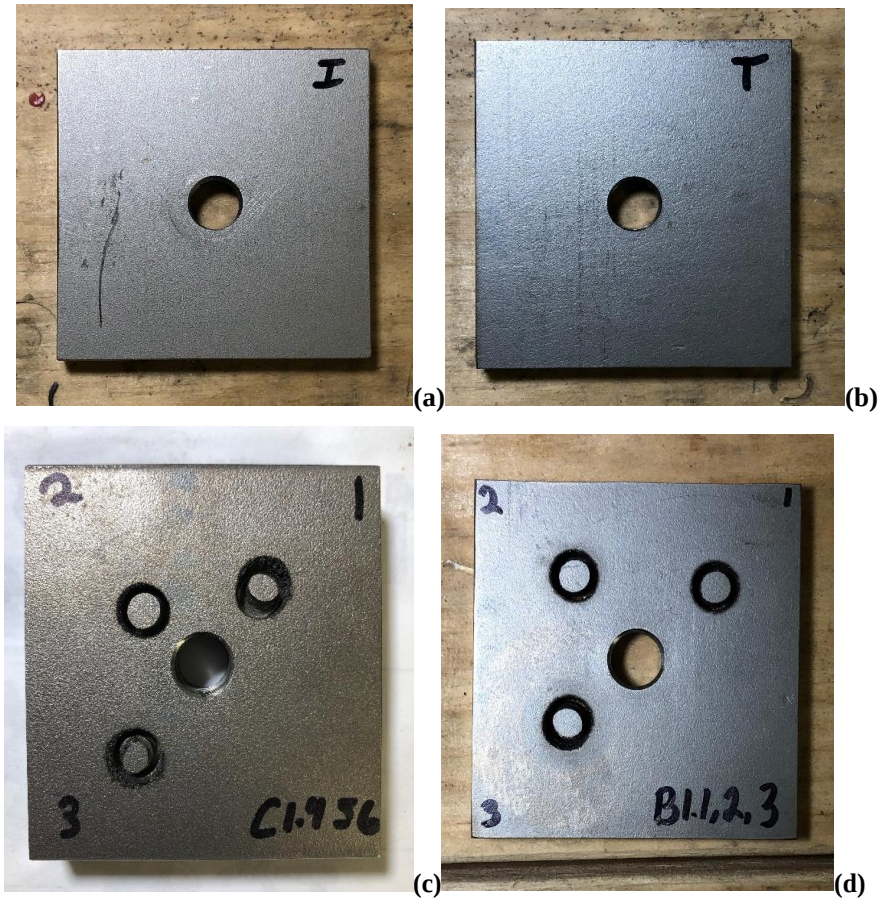

(a) (b) (c) (d)

Figure 14: Uncut Inconel test coupon (a), uncut titanium test coupon (b), Inconel test coupon after cuts (c), titanium test coupon after cuts (d)

Test coupons are secured in place using a small table vice (figs 15 & 16) to reduce any movement caused by the operator. Once the coupon is in place, the cut parameters must be inputted into the E-Drill™ user interface. The electrode diameter, cut depth, and cut target time are selected for the task. There is a plastic locator piece that is designed to help secure and orient the gun perpendicular to the coupon. This locator piece also aids in forming a chamber for the dielectric fluid to flow into and out of the system. Because of the fluid flowing through the locator, there is a rubber gasket fitted to the bottom face of the locator to form a watertight seal. Without this seal, dielectric fluid will leak onto and around the workpiece, reducing the operating water pressure and, in turn, the performance of the tool.

Figure 15: E-Drill locator piece and test piece secured in vice

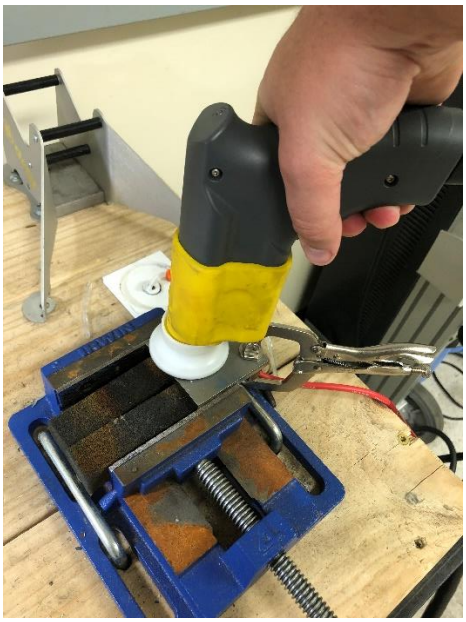

Figure 16: E-Drill and vice in operational configuration

3.2 Design of Experiment

The purpose of this study is to investigate the effects of electrode material and parent material, on electrode wear, resulting in an experiment with 4 parameter tests with 3 cuts per test. The electrode materials were chosen due to their availability, cost, and commonality in EDM use. The depth of cut was chosen to be .20 in because this was a common cut depth required for aerospace fastener removal. This cut depth also utilizes a substantial amount of the stroke of the gun, giving more potential for electrode wear. Each electrode material was used to cut .20in deep hole 3 times in titanium and Inconel, resulting in 12 total cuts.

Once a cut is ready to be made, the test coupon is secured in place via table vice, hole depth, cut type, and material is inputted into the E-Drill™ UI. A fresh electrode is installed on the tool and the grounding clamp is attached to the test coupon. When these steps are complete, the operator begins the test cut by positioning the tool in the proper location, firmly presses the tool against the coupon to form a watertight seal and activates the tool. Cut time can vary greatly depending on parent material, electrode material, and cut depth. Once the machine indicates the cut is complete,

the data recording procedure would be executed. It should be noted that electrical parameters such as current and pulse duration were held constant through all tests. This means that there is likely much room for electrode optimization for each material combination, but that is outside the scope of this study.

3.3 Data Recording Procedure

To record the data, each test had its own note sheet to be filled out. Immediately before the cut was made, the electrode length, diameter, and weight were recorded, as well as the test coupon weight and thickness. For electrode and coupon weight measurement, an OHAUS Model TS4KD Precision Standard balance was used. This scale has a range of 4000 grams with a resolution of 0.1 grams or a range of 400 grams with a resolution of 0.01 grams. Immediately after the cut was made, cut time, coupon weight, electrode weight, electrode length, and any notable comments were recorded for consistency and accuracy. The cut depth measurement had notable error involved due to the imperfect hole made by the electrode, and the placement of the calipers. The calipers used had a bias error of .0005 in. Each individual cut had a unique “task ID” attached to it and each electrode was labeled accordingly, so all data can easily be referenced later. Once all the test cuts were made, the data note sheets were transferred into a spreadsheet format to make the data more organized and easily analyzed.

CHAPTER IV

RESULTS

In this chapter, a discussion of the experiment results is given with respect to the chosen parameters. These parameters are cut time (t), cut rate (μ_h), volume removal ratio (ζ), and volume removal rate (μ_v). For visual representation of each parameter, combination charts are used, seen in Table 1.

Table *2* through table 5 are the mean results of the study, along with the relevant material properties. Due to the nature of the experiment and how measurements were taken, there is potential error introduced into the experiment that should not be ignored. These error sources are mostly human error in the use of the E-Drill™ by not holding the tool perfectly normal to the surface, and hand measurements with the calipers. But there are other sources of error outside of

human control such as the deposition of slag onto the electrode and uneven electrode wear (fig *18*) causing difficulty in measurement. Specifically, the slag deposition can contribute to length measurement with the calipers, and in extreme cases, the measured mass of the electrode could potentially be impacted. These factors resulted in the decision to use standard deviation and mean for statistical analysis of each data set.

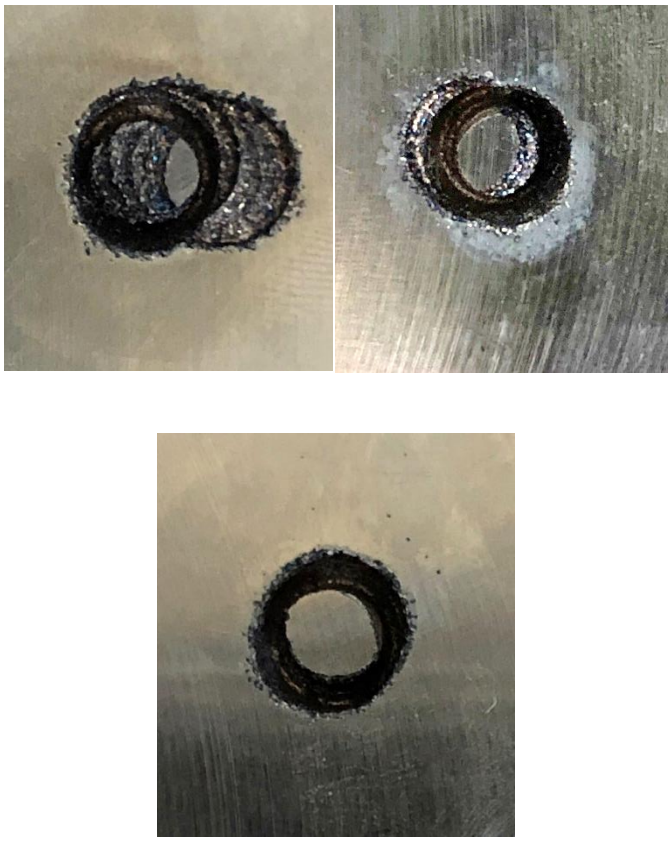

Figure 17: Variation in Completed Titanium Cuts with Copper Electrode. Note the visible copper deposits in the top right image.

Figure 18: Example of Uneven Copper Electrode Wear

Table 1: Properties of materials used [1]

Material	**Electrical Resistivity (ohm-cm)**	**Melting Temperature (F)**	**Thermal Conductivity (BTU/hr-ft²-°F)**	**Density (g/cm^3)**
Brass	2.32E-08	1700	69.33	8.49
Copper	6.69E-09	1980	231	8.94
Titanium	1.69E-07	3000	12.65	4.5
Inconel	4.06E-07	2500	79	8.5

Table 2: Copper electrode test results

	t (s)	μ_h (in/s)	ζ	μ_v (cm^3/s)	Electrical Resistivity (ohm - in)	Melting Point (F)	Thermal Conductivity (BTU/hr-ft²-°F)
Inconel	145	0.00142	0.109	0.0016	4.06E-07	2500	79
Titanium	245	0.000695	0.00219	0.000726	1.69E-07	3000	12.65
% Difference	51.59%	68.71%	192.14%	73.94%	82.19%	18.18%	144.79%

Table 3: Brass electrode test results

	t (s)	μ_h (in/s)	ζ	μ_v (cm^3/s)	Electrical Resistivity (ohm - in)	Melting Point (F)	Thermal Conductivity (BTU/hr-ft²-°F)
Inconel	44.5	0.00436	0.273	0.00348	4.06E-07	2500	79
Titanium	47.4	0.00439	0.166	0.003737	1.69E-07	3000	12.65
% Difference	6.46%	0.67%	48.66%	7.12%	82.19%	18.18%	144.79%

Table 4: Inconel workpiece test results

	t (s)	μ_h (in/s)	ζ	μ_v (cm^3/s)	Electrical Resistivity (ohm - in)	Melting Point (F)	Thermal Conductivity (BTU/hr-ft^2-°F)
Brass	44.5	0.00436	0.273	0.00348	2.32E-08	1700	69.33
Copper	144.8	0.00142	0.109	0.0016	6.69E-09	1980	231
Percent Difference	106.02%	101.62%	85.61%	75.21%	110.53%	15.22%	107.66%

Table 5: Titanium workpiece test results

	t (s)	μ_h (in/s)	ζ	μ_v (cm^3/s)	Electrical Resistivity (ohm - in)	Melting Point (F)	Thermal Conductivity (BTU/hr-ft^2-°F)
Brass	47.4	0.00439	0.166	0.003737	2.32E-08	1700	69.33
Copper	245	0.000695	0.00219	0.000726	6.69E-09	1980	231
Percent Difference	135.22%	145.33%	194.79%	134.92%	110.53%	15.22%	107.66%

4.1 Cut Time (t)

The cut time parameter was measured directly on the E-Drill™ machine. It is a quick and simple method to determine electrode performance by the operator. Cut time is especially significant due to its potential impact on economical savings within the MRO industry. Since a huge driving

factor for this technology is time savings, the electrodes that can do the removal process in the quickest time would likely be the most desirable. For this study, cut time is also used to calculate other parameters nominalized by time. Statistical data and measurement results can be seen in Table 6. Figures 19 and 20 compare workpiece electrical resistivity to cut time. Copper produced cut times of up to 135% longer than brass did at the same cut depth. This lower cut time in brass could play a role in the brass data quality vs. copper data quality because at low cut times, operator fatigue is less of an issue, resulting in a higher quality cut. An interesting observation made is that the copper electrode cut time was largely affected by the change in parent material, while the brass electrode cut time remained mostly constant. Another notable observation is the consistency in cut time. Aside from one copper – titanium cut, the cut time has a relatively small standard deviation.

Table 6: Cut time statistical data

Electrode - Parent Material	Mean t	Standard Dev.	Relative Standard Dev. (%)	Percent Difference
Brass - Titanium	47.43	0.91	1.91%	135.22%
Copper - Titanium	245.47	51.24	20.88%	
Brass - Inconel	44.47	6.31	14.20%	106.02%
Copper - Inconel	144.80	5.90	4.08%	

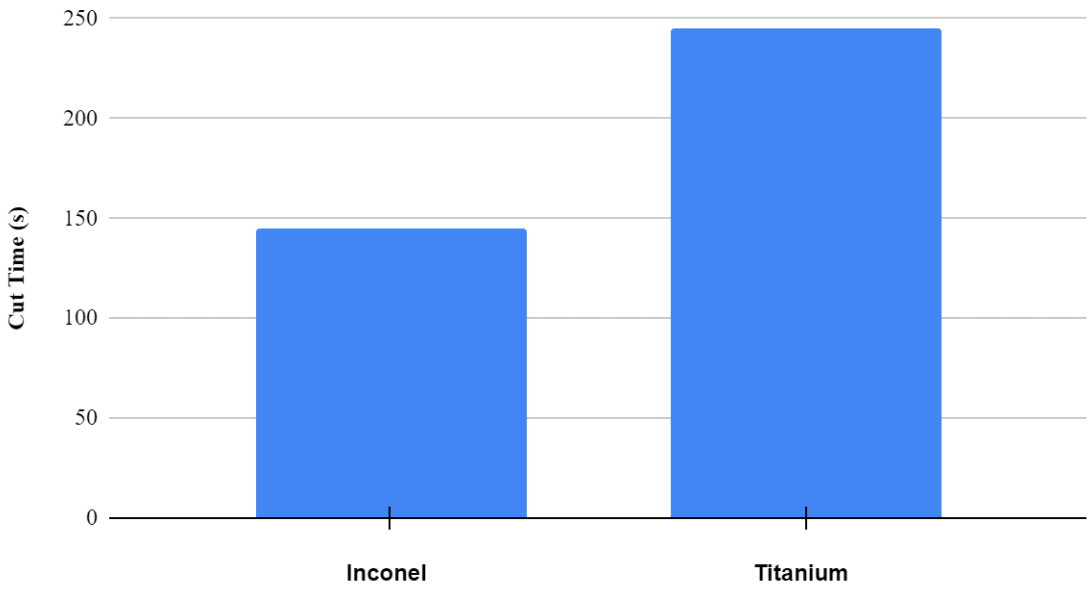

Figure 19: Copper electrode cut time

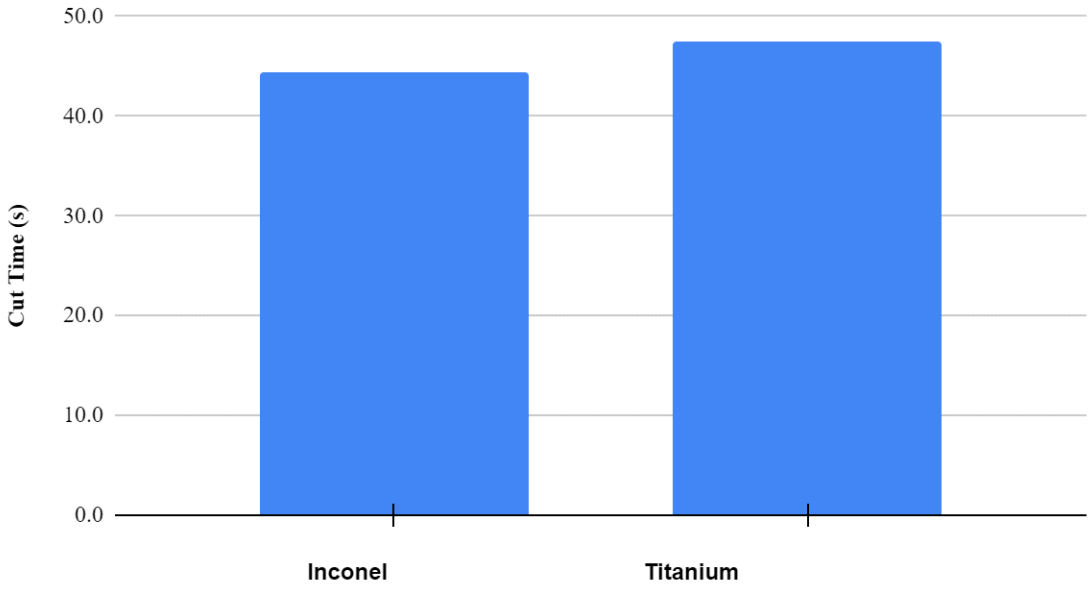

Figure 20: Brass electrode cut time

4.2 Cut Rate

Cut rate is the actual depth of cut divided by the total cut time. In the case of producing deep cuts in a material, the cut rate is a useful metric to aid in predicting the necessary amount of time needed for a given number of those cuts. Since time savings is a driving factor for this technology, cut rate is of great importance to this tool. Figures 21 and 22 show the results of cut rate to workpiece thermal conductivity. Using the reasoning from above, thermal conductivity of the workpiece would be directly related to the cut rate of the tool. The results from the copper electrode follow this reasoning with the Inconel workpiece producing higher cut rate compared to titanium. In fact, the copper electrode cut rate showed a direct correlation to electrical resistivity and thermal conductivity, but an inverse correlation to melting temperature, which is expected. Contrarily, the brass electrode cut rate does not change from Inconel to titanium workpieces. Table 7 shows that the brass cut rate was at least 100% greater than the copper cut rate. It is not known why brass cut rate would not be affected by the workpiece material when the copper was largely affected by it.

A possible cause of the disparity between copper and brass electrodes could be the deposition of slag on the electrodes. Figure 23 shows the difference in slag deposition onto the electrodes. The copper electrode visibly has a large amount of slag build up on the working surface, and the brass electrode does not have much at all. This slag layer is thought to play a role in the performance and life of EDM electrodes. Not much is known about this layer, but it occurs in most EDM processes. The slag material properties could aid in increasing electrode life if it acts as a protective coating with higher conductivity or melting resistance. However, the slag might also have a negative effect on the cutting rate of the electrode.

Table 7: Cut rate statistical analysis

Electrode - Parent Material	Mean (in/s)	Standard Dev.	Relative Standard Dev. (%)	Percent Difference
Brass - Titanium	0.0044	0.000574	13.05%	145.33%
Copper - Titanium	0.0007	0.000185	25.69%	
Brass - Inconel	0.0044	0.000739	16.67%	101.62%
Copper - Inconel	0.0014	0.000189	13.25%	

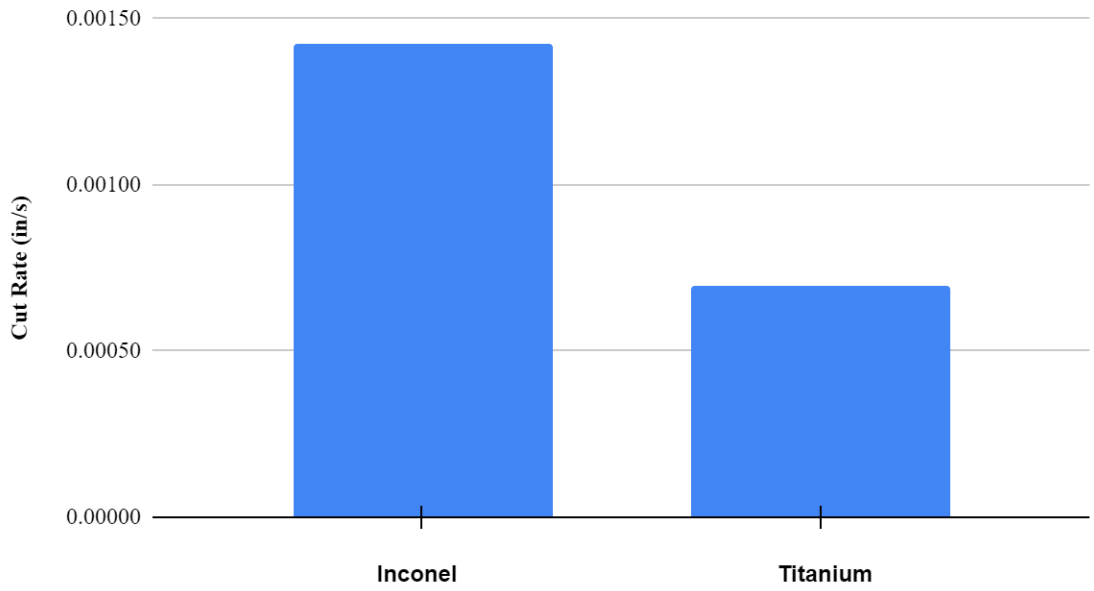

Figure 21: Copper electrode cut rate

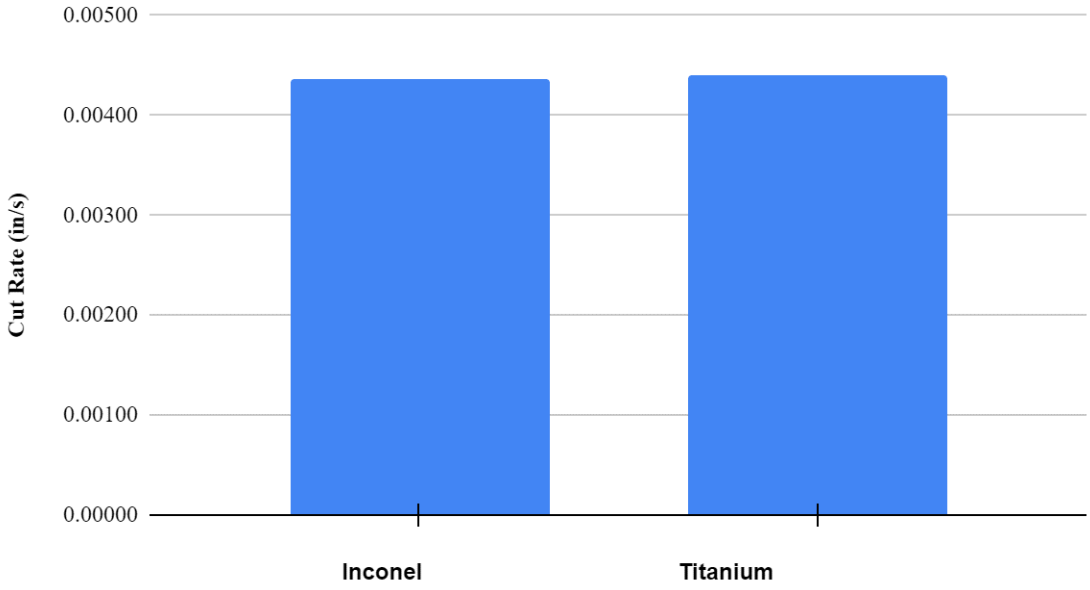

Figure 22: Brass electrode cut rate

Figure 23: Copper electrode (left) has much more slag than the brass electrode (right)

4.3 Volume Removal Rate (μ_v)

Volume removal rate is the volume of workpiece material removed divided by cut time. Volume is used in place of mass because when comparing the performance of two different materials with a significant difference in density, the results may not necessarily correctly indicate which

material performed better. Using volume removal rate as opposed to cut rate from above also considers the possibility of one electrode removing a larger cross-sectional area than another.

Volume removal rate of the copper electrodes changed with workpiece material. Titanium resulted in a lower value than Inconel cuts. However, using brass electrodes, titanium resulted in a 7% increase in volume removal rate over Inconel.

Table 8: Volume removal rate statistical data

Electrode - Parent Material	Mean (in^3/hr)	Standard Dev.	Relative Standard Dev. (%)	Percent Difference
Brass - Titanium	0.821	0.088	10.68%	134.92%
Copper - Titanium	0.160	0.055	34.51%	
Brass - Inconel	0.765	0.054	7.07%	75.21%
Copper - Inconel	0.347	0.028	7.97%	

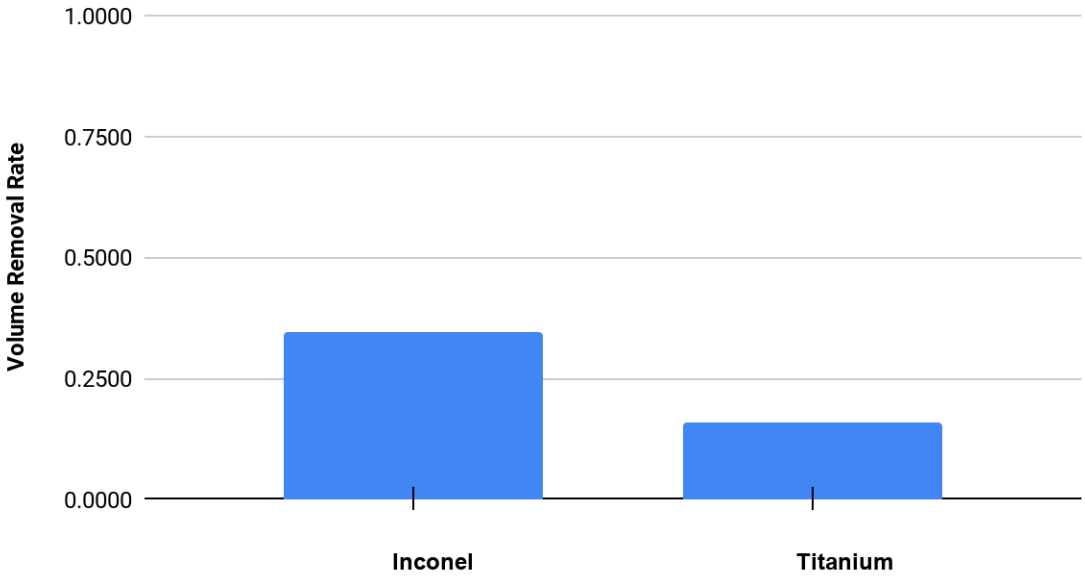

Figure 24: Copper electrode volume removal rate

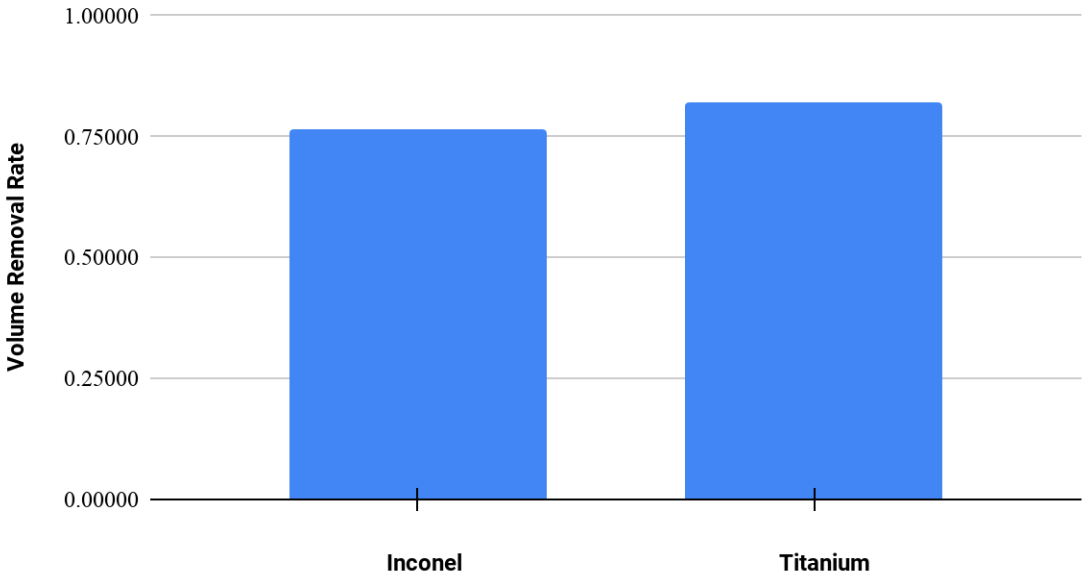

Figure 25: Brass electrode volume removal rate

4.4 Volume Removal Ratio (ζ)

Volume removal ratio is the ratio of electrode volume lost to parent material volume removed. Similar to the volume removal rate, without considering the density of the individual materials, the η_m could be misrepresenting the results, especially if there is a significant disparity between electrode and parent material density. This parameter could be a useful factor in designing electrode geometry for a particular task and material.

Due to the small values at hand, the RSD is sensitive to small changes. Even with this increased sensitivity, three of the data sets were of reasonable value. On the copper – titanium chart in Figure *28*, the negative electrode wear can be seen, which is likely a non-uniform process and results in the large RSD. This is a similar observation that McCain had for cuts into titanium when the electrode increased in mass. It is worth noting that this is the only parameter for brass that had a notable change from Inconel to titanium. Also, no brass cut produced a near zero volume removal ratio like copper did.

Table 9: Volume removal ratio statistical data

Electrode - Parent Material	Mean	Standard Dev.	Relative Standard Dev. (%)	Percent Difference
Brass - Titanium	0.17	0.01	7.58%	194.79%
Copper - Titanium	0.0022	0.02	1635.84%	
Brass - Inconel	0.27	0.05	17.35%	85.61%
Copper - Inconel	0.11	0.0014	1.29%	

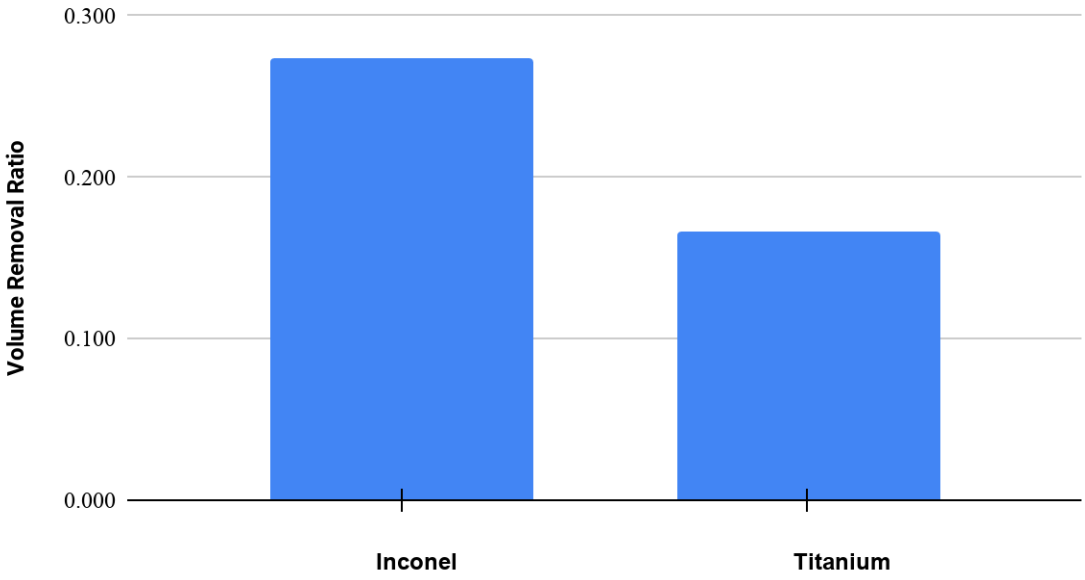

Figure 26: Brass electrode volume removal ratio

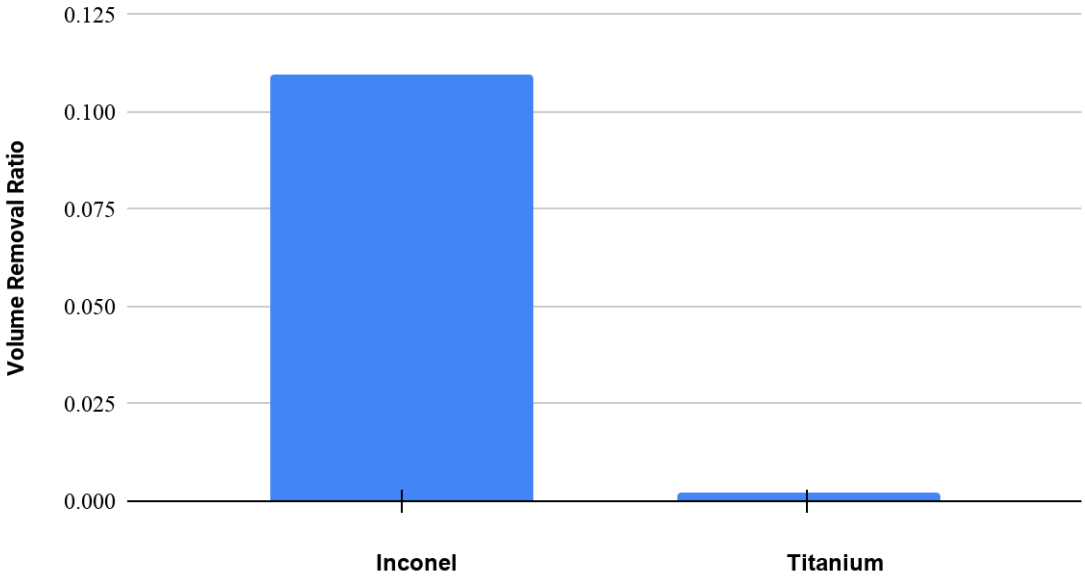

Figure 27: Copper electrode volume removal ratio

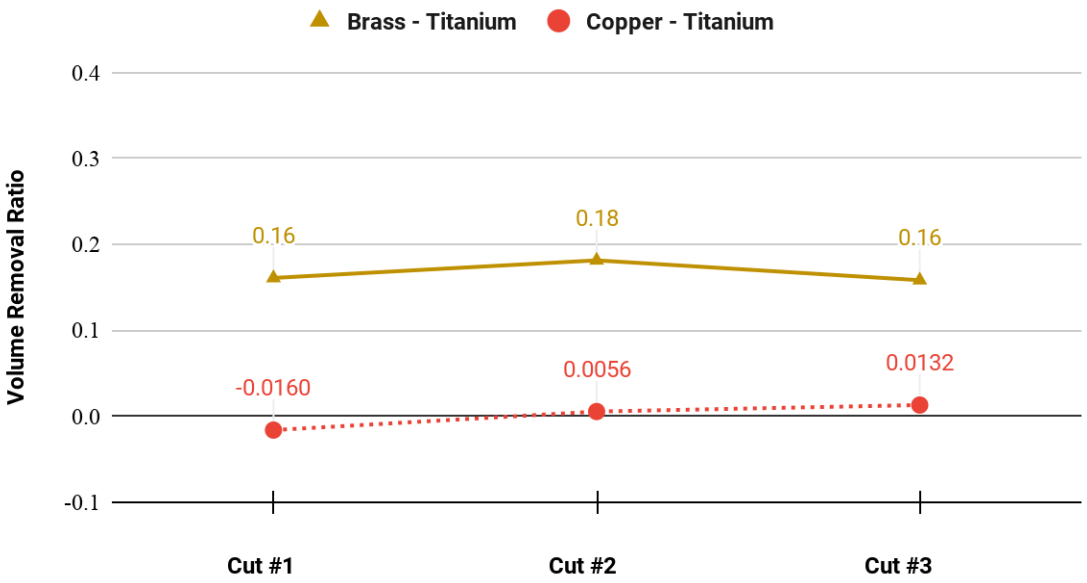

Figure 28: Electrode volume removal ratio in titanium

4.5 Uncertainty Analysis

The data that was acquired was gathered or calculated through simple methods, and there are a low number of data points. This allows for a very simple uncertainty analysis to be used. The uncertainty analysis that was utilized in this study was simple relative standard deviation (RSD). There were some data sets that resulted in very high RSD (over 1000%), but this is caused by the low number of data points and the fact that many values were of very small magnitude, making the RSD extremely sensitive to the slightest change in data magnitude. This is especially true in the copper – titanium tests where negative electrode wear was observed. The fact that slag was depositing onto the electrode results in an even more non-uniform electrode surface and thus very high RSD.

CHAPTER V

RESULTS ANALYSIS

5.1 Correlation to McCain's Results

This section will compare the results of the electrode material study, to McCain's [15] electrode wear study results. McCain's data set does not include the same cut depth, so extrapolation must be done using the provided fitted curve equations. The data set formed by McCain will be referred to as the base data.

McCain's experimentation resulted in a linear relationship between cut time and cut depth. This is expected as the cutting rate of an electrode should remain somewhat stable throughout the process. The data recorded stopped at a max cut depth of .15in. Using a line of best fit for each parent material seen in figs 29 and 30, the data can be extrapolated to reach the new cut depth for comparison across materials. The extrapolated data point is indicated by the black star on the line. Doing so results in predicted cut times of 47.94s for Inconel, and 67.6s for Titanium. The predicted cut times are using an equation formed from the use of electrodes of a different material, said material will be referred to as the base material. When comparing the brass cut time to the base material cut time in table 10, Inconel parent material is quite close in

performance. When brass is cutting into titanium, it appears to make the cut even faster than the base material. On the contrary, the copper electrodes produced significantly longer cut times than the base data predicted. Although the base electrodes are more similar in composition to the copper electrodes, this difference is perhaps influenced by the greater deposition of slag onto the copper electrodes leading to reduced cutting abilities.

Table 10: McCain cut time vs cut depth - Inconel

	Predicted Mean Time	Mean Time Copper	% Diff	Mean Time Brass	% Diff
Inconel	47.94	144.8	100.51%	44.47	7.51%
Titanium	67.6	245.47	113.63%	47.43	35.07%

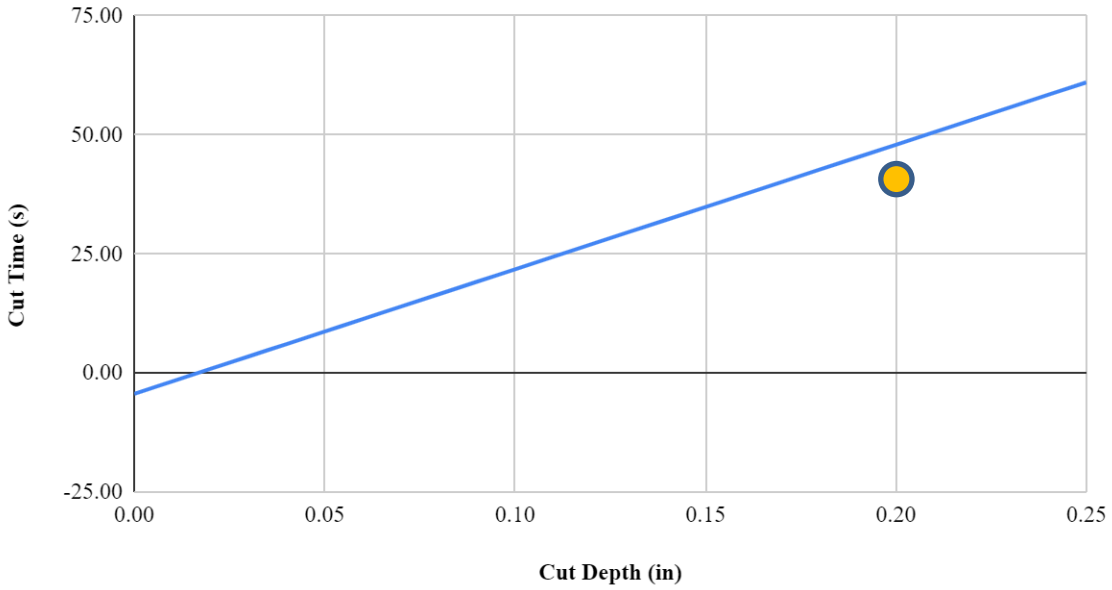

Figure 29: McCain cut time vs cut depth - Inconel

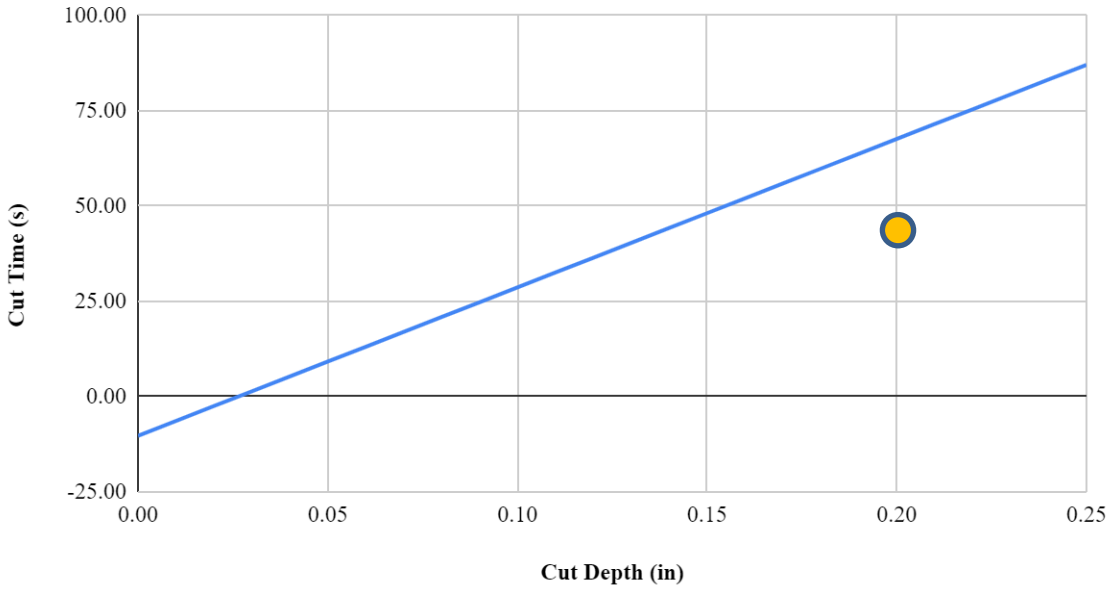

Figure 30: McCain cut depth vs cut time – Titanium

There is only volume removal ratio base data for Inconel parent material, therefore this paragraph will not mention titanium. The base data best fit curve is an exponential curve seen in fig 31. The copper electrode ζ values are very close to the predicted values from the base data. However, the same is not true for the brass electrodes as the data point is far outside the range of this chart.

Table 11: McCain volume removal ratio vs cut depth - Inconel

	Predicted Mean Ratio	Mean Ratio Copper	% Diff	Mean Ratio Brass	% Diff
Inconel	0.1140	0.11	3.57%	0.27	81.25%
Titanium	N/A	N/A	N/A	N/A	N/A

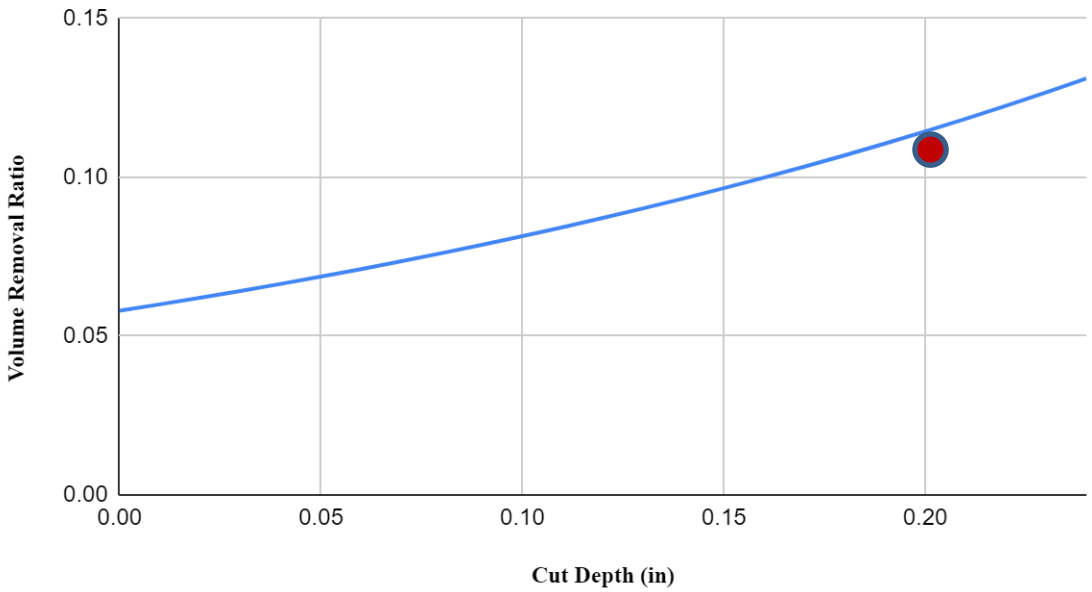

Figure 31: McCain volume removal ratio vs cut depth - Inconel

5.2 Material Properties discussion

The material properties of the electrode as well as the workpiece can impact the performance of the E-Drill™. There are likely many factors at play that make it very difficult to isolate and capture the effects of material properties.

Electrical resistivity of a material could have an impact on the erosion properties. If electrical resistivity is increased, a greater amount of heat is generated from the electrical current, causing the material to heat up more quickly. This could perhaps cause a workpiece with greater electrical resistance to erode more quickly than one with lower electrical resistance. This behavior can be seen in the copper electrode cuts. Inconel has greater electrical resistivity than titanium and resulted in shorter cut times and faster cutting rates.

The melting temperature of a material could impact performance of an electrode especially considering the EDM process utilizes melting the target material. A higher melting

temperature could result in a longer cut time and slower cutting rate because it could take more time to reach that temperature. Once again, copper produced results that agree with this reasoning. Titanium has a higher melting temperature and took longer to cut than Inconel.

The performance of a material could be influenced by thermal conductivity. If thermal energy can be more easily transferred into the workpiece, then it could potentially erode more quickly. This trend is seen in the copper electrodes with a decrease in thermal conductivity from Inconel to titanium and a decrease in cut rate.

5.3 X-Ray Fluorescence Results

X-Ray Fluorescence (XRF) is a technique used to determine the composition of a given material by analyzing the secondary X-Rays emitted from the sample while being excited from an initial X-Ray source. The results of XRF produce data tables that can be analyzed to show the percent make up of each element in the sample.

Two electrodes were analyzed using XRF, one copper-titanium electrode and one brass-titanium electrode. Tables 12 and 13 show the XRF results. The copper, zinc, aluminum, titanium, lead, and vanadium are all expected elements as those are known to be in the titanium alloy or the electrodes already. However, the calcium, potassium, and iron are not known to be in any of the samples, so they must be coming from an external source. The only material used in this study that had an unknown composition was the tap water used for the dielectric fluid. The tap water could have the iron, calcium, and potassium present from the water supply, and it was not being filtered out by the E-Drill onboard water filters. There is no other known source for these elements.

The copper electrode sample showed to have approximately 50% more aluminum than the brass electrode, and nearly 10 times as much titanium deposition. This does agree with the previous observation of the copper electrodes growing in some cases. There could be an electrical galvanic interaction between the lead or zinc content in the brass with the titanium coupon, allowing increased erosion.

Table 12: Copper - Titanium electrode XRF results

Element	Percent Composition (%)
Copper	68.78
Aluminum	22.15
Titanium	3.62
Calcium	3.05
Potassium	1.73
Vanadium	.672

Table 13: Brass - Titanium electrode XRF results

Element	Percent Composition (%)
Copper	50.95
Zinc	25.96
Aluminum	14.70
Lead	3.46
Potassium	2.88
Calcium	1.648
Titanium	.365
Iron	.036

CHAPTER VI

CONCLUSIONS

This chapter summarizes the results, observations, and future recommendations for the E-Drill™ electrode wear study.

6.1 Summary & Observations

This study examined the effects of electrode material on electrode wear during the E-Drill™ EDM process. Other studies have investigated process parameters such as voltage and current, active discharge time, depth of cuts, and even electrode material in micro-EDM. Macro EDM hole drilling using a handheld tool is still a young technology and there is much to be discovered. The results from this study provided a wide range of observations. Brass electrodes had a notably higher wear rate than copper, regardless of the specific parameter considered. However, the brass had a superior machining speed (μ_m, μ_h, t) compared to copper at the cost of greater electrode wear. So, if cut time is a critical factor, brass appears to be a better choice of electrode material. Although, electrical parameters are not taken into consideration in this study and are held constant, so there is possibly some electrical process parameter optimization to be done to fine tune each electrode material. This also means that the default settings used to make these cuts were likely more optimized for brass electrodes, which would explain the difference in performance. This still does not offer any explanation for some of the other key observations made.

The copper electrodes had a notably higher amount of slag deposition when compared to the brass electrode. Not much is known about this mechanism in the EDM process, but it has been observed in many other studies. In S. Ahmed's study [4], it was proposed that the slag or "black layer" is from pyrolysis of the dielectric fluid used, which was kerosene. Pyrolysis is when an organic compound is decomposed in the absence of oxygen [22]. In the current study, the dielectric fluid used is deionized water, so the pyrolysis of said fluid is not a possibility. Regardless of the origin, it is thought that the slag reduces electrode erosion, possibly from a higher melting temperature or electrical properties. However, there is no plausible reason for the different amounts of deposition from the copper to the brass electrode. This is a phenomenon that should be studied further.

It was observed that the copper electrodes were less consistent than brass during a cut. The results from the brass proved to be somewhat predictable and produced desirable cut finishes. On the contrary, the copper electrodes tended to "drift" around throughout the cutting process as can be seen in the above cut images. This could be from operator fatigue during the long operation times upwards of 4 minutes. The operator could have unknowingly been moving the tool while applying pressure. Copper electrodes would "buck" often, indicating the electrode is contacting the workpiece, causing the tool to shift. Slag deposition could be causing electrical conductivity problems which in turn results in electrodes contacting the workpiece. This problem has not been documented previously and is likely exclusive to handheld EDM drills since most EDM drills are rigid like a drill press.

When extrapolating McCain's cut time data from the best fit curves, the resulting predicted time more accurately predicted the brass electrode time and was vastly undershooting the copper electrodes' times. This is unexpected since McCain's electrodes had a high copper content, although not pure.

6.2 Future recommendations

As mentioned previously, a useful future study would be to investigate slag deposition. Why slag is deposited more on the copper than the brass electrodes. If this slag deposition could be better understood, an optimized electrode to parent material match could possibly be made. To do this, one could vary electrical process parameters and evaluate slag with respect to voltage, current, and pulse duration. Another way of evaluating the slag, would be varying materials with known electrical and thermal conductive properties for both the parent material and electrode. A material analysis such as x-ray diffraction could help determine the origin of the slag and allow one to focus on a narrower section of this subject and possibly determine how to further improve electrode performance.

The copper electrodes were extremely inconsistent as mentioned above. The electrode drifted during the cut causing multiple cut paths, or non-uniform cuts. It is unknown if this was caused by operator fatigue with the long cut times, a dielectric fluid pressure issue, or electrical issue. If the drill could be mounted to a rigid frame so that it is locked in place, operator fatigue would not be a factor.

REFERENCES

[1] (n.d.). Retrieved from www.matweb.com: www.matweb.com

[2] (n.d.). Retrieved march 2021, from manufacturing guide: https://www.manufacturingguide.com/

[3] Abbas, N. M. (2007). A Review on Current Research Trends in Electrical Discharge Machining (EDM). *47*(7-8).

[4] Afzaal Ahmed, M. T. (2020). Ultrafast drilling of Inconel 718 using hybrid EDM with different electrode materials. *The International Journal of Advanced Manufacturing Technology*.

[5] Ali, S. M. (2019). Influence of Electrodes and Parameters on Micro-. *International Conference on Engineering Technology and their Applications*.

[6] Cheol-Soo Lee, E.-Y. H.-M.-H.-W. (2015). Electrode wear estimation model for EDM drilling. *Robotics and Computer Manufacturing*.

[7] Copher, G., Harimkar, S., Rouser, K., McCain, C., & Velasco, D. (n.d.). Microstructure effects of electrical discharge machining drill on aerospace super-alloys. *journal of materials engineering and performance (In review)*.

[8] *Discharge Gap*. (n.d.). Retrieved from EDM Tips: https://www.edm.kd-solution.com/en_edm08.html

[9] *EDM drill coin*. (n.d.). Retrieved from novick edm: http://blog.novickedm.com/wp-content/uploads/2018/03/drill-coin-novidrill.jpg

[10] *EDM drilling*. (n.d.). Retrieved from novick edm: https://blog.novickedm.com/wp-content/uploads/2017/09/EDM-drilling-1.jpg

[11] Fu, Y., Miyamoto, T., Natsu, W., Zhao, W., & Yu, Z. (n.d.). Study on Influence of Electrode Material on Hole Drilling in Micro-EDM. *18th CIRP Conference on Electro Physical and Chemical Machining*.

[12] Hasc¸alık, A., & C¸ aydas, U. (2007). Electrical discharge machining of titanium alloy (Ti–6Al–4V). *ELSEVIER*.

[13] *History of EDM*. (n.d.). Retrieved March 2021, from www.edmmachining.com: http://www.edmmachining.com/history_of_edm.htm

[14] IDS Machining. (n.d.). *EDM Machining Process & Techniques*. Retrieved April 6, 2021, from http://www.edmmachining.com/default.htm

[15] McCain, C. (2020). *Electrode Erosion of an Electrical Discharge Machining Drill for Aerospace Fastener Removal.* Master's Thesis.

[16] Misbah Niamat, S. S. (2020). Effect of Different Dielectrics on Material Removal Rate, Electrode Wear Rate and Microstructures in EDM. *The International Journal of Advanced Manufacturing Technology*.

[17] Patrick. (n.d.). *HOW TO DRILL A 0.2 MM DIAMETER HOLE IN TOOL STEEL*. Retrieved from NOVICK: https://blog.novickedm.com/

[18] Ravasio, G. D. (2019). Investigation on the Effects of Exchanged Power and Electrode Properties on Micro EDM Drilling of Stainless Steel.

[19] Skrabalak, G. (2018). Influence of electrode tool length on the micro EDM drilling performance. *19th CIRP Conference on Electro Physical and Chemical Machining*.

[20] Sommer, C., & Steve, S. (n.d.). *Complete EDM Handbook.* Houston, TX: AdvancePublishing.com.

[21] Voort, G. F. (1999). Metallography Principles and Practice. *ASM International*.

[22] *what is pyrolysis*. (n.d.). Retrieved from www.ars.usda.gov: https://www.ars.usda.gov/northeast-area/wyndmoor-pa/eastern-regional-research-center/docs/biomass-pyrolysis-research-1/what-is-pyrolysis/

APPENDICES

APPENDIX A: EXPERIMENTAL SETUP

Acquire all tools needed for this experiment, according to the supply list provided below, before beginning any setup.

1.1. Perfect Point EDM E-Drill ™ Mobile Service Unit (MSU) in Richmond Hill 165CA

1.2. Proper breaker box and outlet, 30A and 240V

1.3. Work bench

1.4. Tap water

1.5. E-Drill ™ Electrode

1.6. E-Drill ™ Hand-Held Terminal (HHT)

1.7. E-Drill ™ gun

1.8. E-Drill ™ locator

1.9. E-Drill ™ adaptor

1.10. E-Drill ™ guide

1.11. E-Drill ™ grounding clamp

1.12. E-Drill ™ torque-ring wrench

1.13. E-Drill ™ Plastic Fill/Drain container

1.14. E-Drill ™ Drain/Fill Tubing

1.15. Transportation containers for specimens

1.16 Marker for labeling all electrodes and fastener material coupons

1.17. 4-inch vise (attached to work bench) with flat surface for specimens

1.18. Desk lamp

1.19. Paper towels

1.20. Safety glasses for all individuals in room

1.21. Gloves for Operator and Assistant Operator

1.22. Trash can

1.23. Needle-nose pliers

1.24. Small chisel set

1.25. Hammer

1.26. Scale

1.27. Fowler High Precision 52-008 Series Dial Caliper

1.28. OHAUS Model TS4KD Precision Standard Balance

1.29. Computer for inputting data

1.30. AMscope for pictures before and after E-Drill ™ operation

2. A minimum of two people will be needed to complete this experiment.

2.1. An operator to run the machine, position the E-Drill ™ gun, hold the gun during cutting, report the cut time, remove the electrode, report the weight on the scale, and prepare the next cut. This individual will select the settings for the cut and take all necessary pictures. They will also document the cut in a specified laboratory notes document.

2.2. Another person to verify the operator's selection of settings, the positioning of the gun, and the vacuum seal throughout the cutting process. This individual will also use paper towels to wipe away any excess water during and after the operation of the E-Drill ™ and position the light in the optimal position during the removal process. Between cuts, this person will enter the data from the cut (e.g. cut time, electrode weight, etc.) into the data spreadsheet.

2.2.1. One person is required to have a charged cell phone in case of emergencies and is required to call emergency services if necessary.

2.2.2. If instead they are the injured party, then know that it is possible to call emergency services without knowing a phone's unlocking code.

2.3. The operator individual must have current EDM training certificates posted on the wall.

2.4. Any other people present must remain a minimum of five feet from the machine and wear eye protection.

2.4.1. Mark sure all individuals who are not operating the machine recognize and stay behind the marked 5-foot line around the machine and workbench.

3. Prepare E-Drill ™ for operation. (From "Perfect Point E-Drill ™ Quick Start & Maintenance Guide")

3.1. With the E-Drill ™ MSU and HHT installed, and power connected to the Mobile Service Unit (MSU), locate the power switch on the back service panel of the MSU and turn it to the "ON" (up) position.

3.2. If indicated the DI water system tank is empty, follow the procedures below from "Perfect Point Fill System Before Use" document.

3.2.1. Unpack the system and locate the joined clear Drain/Fill Tubing and Plastic Fill/Drain container included with the shipment.

3.2.2. Connect the MSU Power Cord and HHT prior to proceeding.

3.2.3. Insert the ends of the Fill/Drain tube in the VACUUM and PRESSURE Ports in the back of the MSU. Fill the Plastic Container with approximately 2 Gal. of clean tap water. Submerge the opposite end of the tubing in the water. Ensure the end the tubing will remain submerged throughout the following procedures or air will be introduced into the system and bleeding procedures will take longer than necessary.

3.2.4. Power up the system. It will take approximately 30 seconds for the HHT to load the system program. Once the terminal screen is lit and menus appear, proceed to Step v.

3.2.5. Use the HHT to access the system Maintenance screen. Run the “Top Off” procedure to charge the dielectric system. The vacuum pump will start, drawing water into the system until the HHT indicates the tank is full and the pump shuts off automatically.

3.2.6. Next, run “Empty Sediment Tank” routine to purge the system of air, while taking care to hold the end of the fill drain tube submerged in the container. The pressure pump will start, expelling water from the system until the HHT indicates the tank is empty and the pump shuts off automatically. A popup screen will appear on the HHT asking if the Sediment Tank is being cleaned. Select “NO”. Run the “Top Off” procedure once more to fully fill the system. If you have reason to believe that all the air has not been bled from the fluid system, repeat Step vi.

3.2.7. When connecting an E-Drill ™ gun to the system, it is good practice to bleed the E-Drill ™ umbilical before use. Connect the E-Drill ™ Umbilical Cable to the MSU. Be sure the umbilical VACUUM and PRESSURE lines are installed in their proper locations. Turn the MSU Circuit Breaker “ON”. When the HHT has booted up, navigate to the Maintenance screen. Install an Electrode and its matching Adapter in the E-Drill ™, and completely retract the Electrode using the Retract button.

3.2.8. Press the “Empty Sediment Tank” button on the HHT Maintenance screen; the pressure pump will start. Next; using the empty Plastic Fill/Drain container, depress the E-Drill ™ ground pin against the floor of the container. Allow entrapped air and water flow to escape from the E-Drill ™ tip until a steady flow of water is achieved, then stop the pump by pressing the “Empty Sediment Tank” button again.

3.3. The system will power up and after a few seconds the Hand Held Terminal touch screen will illuminate and display the last fastener entry.

3.4. If the screen of the Handheld Terminal is not illuminated, touch the screen to awaken it. Go to bottom right tab on screen and touch the tab for “Select: Visual”.

3.4.1. Under “Type”, scroll down to and select “Hole” option.

3.4.2. Under “Method”, select the “Flush Head” option.

3.4.3. Under “Material”, select the “Titanium” or “Inconel” options.

3.4.4. For “Head Ø”, select the proper electrode diameter value.

3.4.5. Under “Shank Ø”, select the “13/65 (0.203)” option.

3.5. If the cut depth needs to be adjusted in smaller increments than allowed by “Select: Visual”, then the operator needs to open the “Advanced Mode”.

3.5.1. Begin by pressing the top left corner of the screen followed by the top right corner, within 2 seconds.

3.5.2. Enter the password provided to those who have completed the proper training.

3.5.3. Press the tab titled “Advanced” at the bottom middle of the screen.

3.5.4. Tap the box next to “Cut Depth:” and enter the desired cut depth. Press the “Save” tab at the bottom of the screen.

3.6. Install the proper electrode into the E-Drill ™ and the correct adaptor for the fastener type to be removed.

3.7. E-Drill ™ grounding clamp should be attached to the parent material and connected to the wire hanging from the gun.

3.8. Electrode replacement is when the current electrode is consumed and should be replaced when indicated by a flashing green light on the hand-tool and a message on the Hand Held Terminal. The replacement process is provided below.

3.8.1. Unlock the installed Adapter Tip by gripping and twisting it counter-clockwise (when viewed from the front of the e drill). Then pull the Adapter tip straight out.

3.8.2. Unthread the existing Electrode using the Torque-Ring Wrench by inserting it over the Electrode until it engages the Electrode detents. Remove the Electrode by turning it

counter-clockwise. It may be necessary to advance the electrode: in which case, with system power on, advance the installed electrode completely forward by depressing gun trigger until the Electrode advances fully. When you have reached the forward limit the LED at the top of the E-Drill ™ will illuminate Red and the E-Drill ™ mechanism will stop automatically. If the electrode wont advance, and the system is indicating that the electrode should be replaced, press the green retract button briefly before attempting to advance the electrode.

3.8.3. Hand-thread the replacement Electrode onto the E-Drill.

3.8.4. Retract the Electrode by pressing and holding down the green retract button in the base of the E-Drill ™ grip until the LED in the back of the E-Drill ™ handle illuminates Green indicating the Electrode is fully retracted.

4. Prepare the specimens for operation.

4.1. Measure the height, outer diameter (OD), inner diameter (ID), and weight of the electrode. Then, input all data into the computer.

4.2. Measure the length, width, height, and weight of the fastener material coupon. Then, input the data into the computer.

APPENDIX B: EXPERIMENTAL PROCEDURE

1. Ensure all participants are wearing PPE per safety instructions before starting any part of the experimental procedures.
2. Record both users and any maintenance procedures performed, including both date and time.
3. Before operating further, consult the checklist to ensure no errors occur during experimentation.
4. Next, place the jig on the specimen and clamp them together in the vise, tightening down to ensure the specimen and jig will not move while drilling.
5. To prepare the E-Drill™ gun, place the corresponding adapter for the locator onto the end of the gun.
6. To start the drilling process, grab the E-Drill™ gun in your dominant hand. The pointer finger should lay along the side of the gun and the middle finger should hold the trigger, with the rest holding the handle.
7. Insert the electrode side of the gun into the locator perpendicular to the parent material.
8. Check to make sure there is a green light on the E-Drill™ showing that it is ready to cut. If the light is not green, refer to the Perfect Point E-Drill™ Quick Start and Maintenance Guide.
9. Place your non-dominant hand on top of the gun and apply light pressure, this is to properly seal the end and to ensure a nice, clean cut.

10. Keeping pressure applied, squeeze the trigger with your middle finger to start drilling. Keep holding the trigger until the machine stops cutting.

11. After the EDM is done drilling, leave the gun pressed down for a few seconds then tilt it at a slight angle to allow excess liquid to be vacuumed into the machine

12. Place the gun into the work bench holster and remove the locator from on top of the parent material.

13. Use paper towels to wipe up any excess liquid from the specimen, making sure to dispose of the paper towels in the trash bin.

14. Next, take detailed pictures of the post cut specimen making sure that the eccentricity of the specimen is visible.

15. Use calipers to record detail measurements of the following in English units:

    28.1. Electrode ID and OD

    28.2. Length of the electrode

    28.4. ID and OD of cut

    28.7. Weight of electrode and of the parent material

16. Make sure that all measurements have been recorded and that the transportation cases are stored properly.

17. Repeat all steps, with a new specimen.

VITA

Garner Gene Copher

Candidate for the Degree of

Master of Science

Thesis: EFFECTS OF ELECTRODE MATERIAL ON ELECTRODE EROSION OF ELECTRICAL DISCHARGE MACHINING DRILL

Major Field: Mechanical and Aerospace Engineering

Biographical:

Education:

Completed the requirements for the Master of Science in Mechanical and Aerospace Engineering at Oklahoma State University, Stillwater, Oklahoma in May, 2021.

Completed the requirements for the Bachelor of Science in Aerospace Engineering at Oklahoma State University, Stillwater, Oklahoma in 2019.

Completed the requirements for the Bachelor of Science in Mechanical Engineering at Oklahoma State University, Stillwater, Oklahoma in 2019.

Experience:

Graduate Research Assistant – Oklahoma State University, Stillwater, OK
Graduate Teaching Assistant – Oklahoma State University, Stillwater, OK